Ultra-large nonlinear parameter in graphene-silicon waveguide structures

Christine Donnelly[1] and Dawn T. H. Tan[2,*]

[1]*Stanford University, Stanford, California 94305-4085, USA*
[2]*Engineering Product Development, Singapore University of Technology and Design, 20 Dover Dr., Singapore 138682, Singapore*
[*]dawn_tan@sutd.edu.sg,

Abstract: Mono-layer graphene integrated with optical waveguides is studied for the purpose of maximizing E-field interaction with the graphene layer, for the generation of ultra-large nonlinear parameters. It is shown that the common approach used to minimize the waveguide effective modal area does not accurately predict the configuration with the maximum nonlinear parameter. Both photonic and plasmonic waveguide configurations and graphene integration techniques realizable with today's fabrication tools are studied. Importantly, nonlinear parameters exceeding 10^4 W^{-1}/m, two orders of magnitude larger than that in silicon on insulator waveguides without graphene, are obtained for the quasi-TE mode in silicon waveguides incorporating mono-layer graphene in the evanescent part of the optical field. Dielectric loaded surface plasmon polariton waveguides incorporating mono-layer graphene are observed to generate nonlinear parameters as large as 10^5 W^{-1}/m, three orders of magnitude larger than that in silicon on insulator waveguides without graphene. The ultra-large nonlinear parameters make such waveguides promising platforms for nonlinear integrated optics at ultra-low powers, and for previously unobserved nonlinear optical effects to be studied in a waveguide platform.

OCIS codes: (190.0190) Nonlinear optics; (190.4390) Nonlinear optics, integrated optics; (130.4310) Nonlinear; (160.4330) Nonlinear optical materials.

References and links

1. K. S. Novoselov, A. K. Geim, S. V. Morozov, D. Jiang, M. I. Katsnelson, I. V. Grigorieva, S. V. Dubonos, and A. A. Firsov, "Two-dimensional gas of massless Dirac fermions in graphene," Nature **438**(7065), 197–200 (2005).
2. A. A. Balandin, S. Ghosh, W. Bao, I. Calizo, D. Teweldebrhan, F. Miao, and C. N. Lau, "Superior thermal conductivity of single-layer graphene," Nano Lett. **8**(3), 902–907 (2008).
3. C. Lee, X. Wei, J. W. Kysar, and J. Hone, "Measurement of the elastic properties and intrinsic strength of monolayer graphene," Science **321**(5887), 385–388 (2008).
4. T. Mueller, F. Xia, and P. Avouris, "Graphene photodetectors for high-speed optical communications," Nat. Photonics **4**(5), 297–301 (2010).
5. B. Y. Zhang, T. Liu, B. Meng, X. Li, G. Liang, X. Hu, and Q. J. Wang, "Broadband high photoresponse from pure monolayer graphene photodetector," Nat Commun. **4**, 1811 (2013).
6. M. Liu, X. Yin, E. Ulin-Avila, B. Geng, T. Zentgraf, L. Ju, F. Wang, and X. Zhang, "A graphene-based broadband optical modulator," Nature **474**(7349), 64–67 (2011).
7. J. Gosciniak and D. T. H. Tan, "Graphene-based waveguide integrated dielectric-loaded plasmonic electro-absorption modulators," Nanotechnology **24**(18), 185202 (2013).
8. J. Gosciniak and D. T. H. Tan, "Theoretical investigation of graphene-based photonic modulators," Sci Rep. **3**, 1897 (2013).
9. S. A. Mikhailov, "Non-linear electromagnetic response of graphene," Europhys. Lett. **79**(2), 27002 (2007).
10. S. A. Mikhailov and K. Ziegler, "Nonlinear electromagnetic response of graphene: frequency multiplication and the self-consistent-field effects," J. Phys. Condens. Matter **20**(38), 384204 (2008).
11. E. Hendry, P. J. Hale, J. Moger, A. K. Savchenko, and S. A. Mikhailov, "Coherent nonlinear optical response of graphene," Phys. Rev. Lett. **105**(9), 097401 (2010).

#222438 - $15.00 USD Received 4 Sep 2014; accepted 4 Sep 2014; published 12 Sep 2014

12. H. Zhang, S. Virally, Q. Bao, L. K. Ping, S. Massar, N. Godbout, and P. Kockaert, "Z-scan measurement of the nonlinear refractive index of graphene," Opt. Lett. **37**(11), 1856–1858 (2012).
13. T. Gu, N. Petrone, J. F. McMillan, A. Van Der Zande, M. Yu, G. Q. Lo, D. L. Kwong, J. Hone, and C. W. Wong, "Regenerative oscillation and four-wave mixing in graphene optoelectronics," Nat. Photonics **6**(8), 554–559 (2012).
14. D. T. H. Tan, K. Ikeda, P. C. Sun, and Y. Fainman, "Group velocity dispersion and self phase modulation in silicon nitride waveguides," Appl. Phys. Lett. **96**(6), 061101 (2010).
15. M. Ferrera, L. Razzari, D. Duchesne, R. Morandotti, Z. Yang, M. Liscidini, J. E. Sipe, S. Chu, B. E. Little, and D. J. Moss, "Low-power continuous-wave nonlinear optics in doped silica glass integrated waveguide structures," Nat. Photonics **2**(12), 737–740 (2008).
16. A. C. Turner, M. A. Foster, A. L. Gaeta, and M. Lipson, "Ultra-low power parametric frequency conversion in a silicon microring resonator," Opt. Express **16**(7), 4881–4887 (2008).
17. D. T. H. Tan, P. C. Sun, and Y. Fainman, "Monolithic nonlinear pulse compressor on a silicon chip," Nat Commun. **1**(8), 116 (2010).
18. P. Colman, C. Husko, S. Combrié, I. Sagnes, C. W. Wong, and A. De Rossi, "Temporal solitons and pulse compression in photonic crystal waveguides," Nat. Photonics **4**(12), 862–868 (2010).
19. D. T. H. Tan, "Optical pulse compression on a silicon chip – Effect of group velocity dispersion and free carriers," Appl. Phys. Lett. **101**(21), 211112 (2012).
20. A. Blanco-Redondo, C. Husko, D. Eades, Y. Zhang, J. Li, T. F. Krauss, and B. J. Eggleton, "Observation of soliton compression in silicon photonic crystals," Nat Commun. **5**, 3160 (2014).
21. G. P. Agrawal, *Nonlinear Fiber Optics* (Academic, 1995).
22. I. D. Rukhlenko, M. Premaratne, and G. P. Agrawal, "Effective mode area and its optimization in silicon-nanocrystal waveguides," Opt. Lett. **37**(12), 2295–2297 (2012).
23. M. A. Foster, K. D. Moll, and A. L. Gaeta, "Optimal waveguide dimensions for nonlinear interactions," Opt. Express **12**(13), 2880–2887 (2004).
24. H. Fukada, K. Yamada, T. Shoji, M. Takahashi, T. Tsuchizawa, T. Watanabe, J. Takahashi, and S. Itabashi, "Four-wave mixing in silicon wire waveguides," Opt. Express **13**, 4629–4637 (2005).
H. Yamada, M. Shirane, T. Chu, H. Yokoyama, S. Ishida, and Y. Arakawa, "Nonlinear-optic silicon-nanowire waveguides," Jpn. J. Appl. Phys. **44**, 6541–6545 (2005).
25. E. Dulkeith, Y. A. Vlasov, X. Chen, N. C. Panoiu, and R. M. Osgood, Jr., "Self-phase-modulation in submicron silicon-on-insulator photonic wires," Opt. Express **14**(12), 5524–5534 (2006).
26. M. Dinu, F. Quochi, and H. Garcia, "Third-order nonlinearities in silicon at telecom wavelengths," Appl. Phys. Lett. **82**(18), 2954–2956 (2003).
27. H. K. Tsang, C. S. Wong, T. K. Liang, I. E. Day, S. W. Roberts, A. Harpin, J. Drake, and M. Asghari, "Optical dispersion, two-photon absorption and self-phase modulation in silicon waveguides at 1.5 μm wavelength," Appl. Phys. Lett. **80**(3), 416–418 (2002).
28. T. Wang, N. Venkatram, J. Gosciniak, Y. Cui, G. Qian, W. Ji, and D. T. H. Tan, "Multi-photon absorption and third-order nonlinearity in silicon at mid-infrared wavelengths," Opt. Express **21**(26), 32192–32198 (2013).
29. S. A. Mikhailov and K. Ziegler, "New electromagnetic mode in graphene," Phys. Rev. Lett. **99**(1), 016803 (2007).
30. S. Hong, J. I. Dadap, N. Petrone, P. Yeh, J. Hone, and R. M. Osgood, "Optical third-harmonic generation in graphene," Phys. Rev. X **3**, 021014 (2013).
31. M. L. Nesterov, J. Bravo-Abad, A. Y. Nikitin, F. J. García-Vidal, and L. Martin-Moreno, "Graphene supports the propagation of subwavelength optical soltions," Laser Photon. Rev. **7**(2), L7–L11 (2013).
32. A. V. Gorbach, A. Marini, and D. V. Skryabin, "Graphene-clad tapered fiber: effective nonlinearity and propagation losses," Opt. Lett. **38**(24), 5244–5247 (2013).
33. Y. Li, B. A. Malomed, J. Wu, W. Pang, S. Wang, and J. Zhou, "Quasi-compactons in inverted nonlinear photonic crystals," Phys. Rev. A **84**(4), 043839 (2011).
34. M. A. Foster, A. C. Turner, J. E. Sharping, B. S. Schmidt, M. Lipson, and A. L. Gaeta, "Broad-band optical parametric gain on a silicon photonic chip," Nature **441**(7096), 960–963 (2006).
35. J. Cardenas, C. B. Poitras, J. T. Robinson, K. Preston, L. Chen, and M. Lipson, "Low loss etchless silicon photonic waveguides," Opt. Express **17**(6), 4752–4757 (2009).
36. D. J. Moss, R. Morandotti, A. L. Gaeta, and M. Lipson, "New CMOS-compatible platforms based on silicon nitride and Hydex for nonlinear optics," Nature Photon. **7**(8), 597–607 (2013).
37. X. Liu, R. M. Osgood, Y. A. Vlasov, and W. M. J. Green, "Mid-infrared optical parametric amplifier using silicon nanophotonic waveguides," Nat. Photonics **4**(8), 557–560 (2010).
38. H. Yang, X. Feng, Q. Wang, H. Huang, W. Chen, A. T. Wee, and W. Ji, "Giant Two-Photon Absorption in Bilayer Graphene," Nano Lett. **11**(7), 2622–2627 (2011).
39. B. Corcoran, C. Monat, M. Pelusi, C. Grillet, T. P. White, L. O'Faolain, T. F. Krauss, B. J. Eggleton, and D. J. Moss, "Optical signal processing on a silicon chip at 640Gb/s using slow-light," Opt. Express **18**(8), 7770–7781 (2010).
40. R. M. Osgood, Jr., N. C. Panoiu, J. I. Dadap, X. Liu, X. Chen, I.-W. Hsieh, E. Dulkeith, W. M. Green, and Y. A. Vlasov, "Engineering nonlinearities in nanoscale optical systems: physics and applications in dispersion-engineered silicon nanophotonic wires," Adv. Opt. Photon. **1**(1), 162–235 (2009).

#222438 - $15.00 USD Received 4 Sep 2014; accepted 4 Sep 2014; published 12 Sep 2014

1. Introduction

The use of graphene in diverse fields such as electronics and energy storage may be attributed to its excellent electron mobility [1], high thermal conductivity [2] and mechanical strength [3]. More recently, graphene has been studied for its interesting photonics properties. As a result of graphene's zero bandgap and tunable chemical potential, new paradigms for photodetectors [4,5] and optical modulators have arisen [6–8]. In addition, graphene has recently been theoretically predicted and experimentally characterized to have the largest nonlinear refractive index of any known material [9–13]. Materials with a high nonlinear refractive index are important as they serve as sources from which frequency generation [14–16], temporal pulse compression [17–20] and other nonlinear phenomena can be generated.

The proliferation of silicon nanophotonics over ten years ago was due to a number of factors, including silicon's compatibility with complementary metal oxide semiconductor processes, as well as the ability to engineer nonlinear parameters 5 orders of magnitude larger than those in single mode silica fibers. The discovery of graphene's large nonlinear refractive index serves as another game-changer which could enable new nonlinear effects to be studied. However, current fabrication constraints limit where and how graphene's large nonlinear refractive index can be leveraged.

The design of nonlinear photonic waveguides such as silicon on insulator and silicon nitride waveguides typically involves the minimization of the effective mode area. In these cases, the waveguide core material serves as the main contributor to the nonlinear effects. In this paper, we show that this approach leads to large inaccuracies in the design of graphene-integrated waveguides for nonlinear optics. Because the graphene layer is very thin, strategies for evaluating the nonlinear parameter differ from approaches used to optimize the nonlinear parameter in waveguides where the core serves as the main nonlinear material. We also study the optimization of graphene integrated waveguide structures for the purpose of maximizing the nonlinear parameter of the hybrid waveguide structure. The ultrahigh nonlinear parameter can thereafter be used for supporting temporal solitons, four wave mixing and pulse compression at power levels significantly lower than those demonstrated in other integrated waveguide platforms. A key observation is that graphene's large nonlinear refractive index enables its host waveguide to have a two to three order increase in the nonlinear parameter as compared to silicon waveguides, even if the graphene sheet is located in the evanescent region of the electric field.

2. Nonlinear optics with graphene

The nonlinear refractive index n_2 (cm^2/W) for a medium is defined by

$$\phi(z) = \beta(\omega)z + \beta_{NL}(I)z = \frac{\omega z(n_o + n_2 I)}{c} \tag{1}$$

where $\phi(z)$ is the total phase for a wave propagating in the z-direction, ω is the frequency of the wave, z is the propagation distance, n_o is the linear refractive index, $\beta(\omega)$ is the wavenumber corresponding to the linear index, I is the field intensity, $\beta_{NL}(I)$ is the nonlinear contribution to the wavenumber, and c is the speed of light in vacuum. The nonlinear index n_2 quantifies the intensity-dependent phase accumulation due to third-order nonlinear effects.

Graphene has been reported to have extremely large nonlinear refractive indices varying between 6 X 10^{-8} cm^2/W (measured at normal incidence using the Z-scan method) [11] and 10^{-9} cm^2/W (theoretically calculated and experimentally verified via in-plane four-wave mixing measurements) [13]. The third order nonlinear susceptibility of graphene at a specific wavelength may also be calculated using [10] $\chi^{(3)} = \frac{\lambda^5 . \alpha^3}{d_{gr} . e^2} . \left(\frac{V^2}{c^2} \right)$, where $\chi^{(3)}$ is the third order nonlinear susceptibility, e is the charge in an electron, and in our case, λ = 1.55μm, α is

#222438 - $15.00 USD Received 4 Sep 2014; accepted 4 Sep 2014; published 12 Sep 2014

the fine structure constant, the thickness of graphene, d_{gr} = 0.36nm and the Fermi velocity, V = 10^6 m/s. This parameter is related to the nonlinear index n_2 via the relation, $n_2 = \frac{3Z\chi^{(3)}}{4n_\omega^2}$, where, ω is the frequency, Z is the intrinsic impedance and n_ω is the linear refractive index of the medium. Calculations using these parameters yields a third order nonlinear susceptibility, $\chi^{(3)} \approx 5 \times 10^{-13}$ esu; the introduction of graphene can thus significantly enhance nonlinear effects even when included in small thicknesses.

In this paper we consider three structures that may be easily integrated using state of the art nanofabrication techniques with graphene-based nonlinear optics for confining electromagnetic power to propagation along a single direction (see Fig. 1):

(1) Channel polymer waveguide consisting of a SU-8 slab on SiO_2 substrate with air as the overcladding. Power confinement occurs due to total internal reflections at the boundary between the relatively high-index SU-8 and its lower-index surroundings, and both the fundamental quasi-TM and TE modes are considered. For nonlinear phase generation, a graphene monolayer is located at the center of the SU-8 slab, at the region of highest mode intensity.

(2) Channel waveguides consisting of a silicon slab on SiO_2 substrate with air as the overcladding. Due to fabrication limitations, the graphene layer in this case is deposited on the top surface of the silicon slab rather than at the center of the waveguide.

(3) Dielectric loaded surface plasmon polartion waveguide (DLSPP) consisting of a dielectric silicon slab covered with a graphene monolayer, followed by 50nm of gold with PMMA overcladding. Such a structure supports the propagation of TM-like surface plasmon polaritons parallel to the interface between the lossy metal and dielectric.

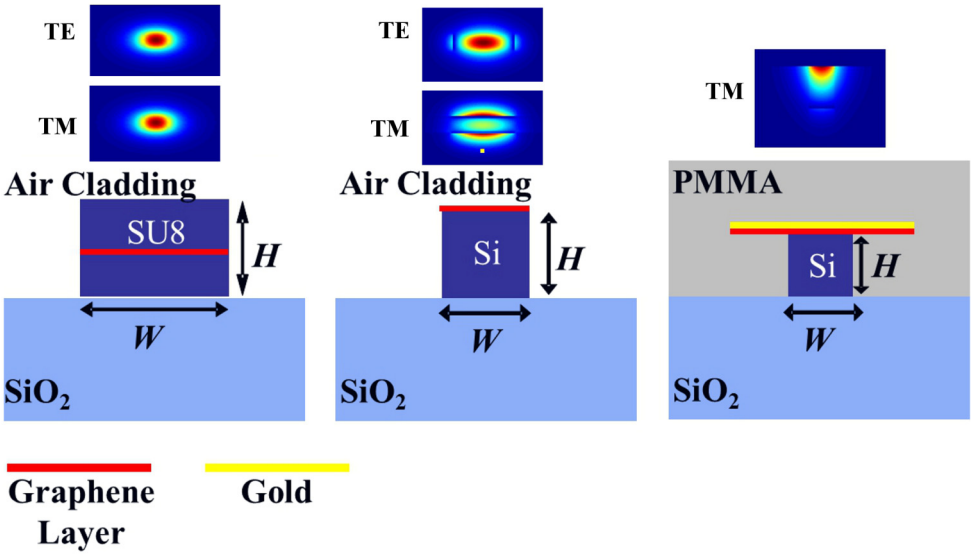

Fig. 1. Schematic of (a) SU8 channel waveguide with graphene monolayer in the center (quasi-TE mode of a typical waveguide is shown), (b) silicon channel waveguide with graphene monolayer (quasi-TE mode of a typical waveguide is shown) and (c) DLSPP waveguide consisting of a silicon core, graphene monolayer and 50nm gold layer (TM mode of a typical waveguide is shown).

#222438 - $15.00 USD Received 4 Sep 2014; accepted 4 Sep 2014; published 12 Sep 2014

The evolution of the normalized electric field amplitude, U(z) subjected to an optical intensity, I along the z-direction due to third-order nonlinear effects is given by, $i\frac{dU}{dz}=\frac{\omega n_2 I}{c}|U|^2 U$, where ω is the frequency, n_2 is the nonlinear refractive index and c is the speed of light in vacuum. This expression, when combined with a consideration of group velocity dispersion effects yields the nonlinear Schrodinger equation [21].

In the case of waveguides, the explicit dependence on modal power, P can be included by rewriting

$$I=\frac{P}{A_{eff}} \tag{2}$$

where the effective area, A_{eff} is given by:

$$A_{eff}=\frac{\left(\iint_D S_z\,dxdy\right)^2}{\iint_D S_z^2\,dxdy} \tag{3}$$

S_z here is the time-averaged Poynting vector and the domain "D" is defined by all core and cladding material in which there is either a propagating or evanescent electric field intensity. Previous studies on the optimization of the nonlinear parameter largely involved minimizing the effective area of the guided mode described by Eq. (3), in silicon on insulator (SOI) channel or slot waveguides, in order to achieve maximum nonlinear effects. In SOI waveguides, a small effective area where the field is tightly concentrated within a small area within the core is needed because the nonlinear refractive index being exploited for the nonlinear effects is that of the silicon core itself. In essence, this generates a large optical intensity within the waveguide [see Eq. (2)]. Since the acquisition of nonlinear phase scales with the optical intensity [as shown in Eq. (1)], this strategy generates the largest nonlinear effects. In slot waveguides, the optical fields are concentrated mainly within the lower index core region, and therefore inserting a lower index material with a high nonlinearity within the core has been the strategy for maximizing the nonlinear parameter of the slot waveguide.

In the case of the slot waveguide, it has recently been shown that merely minimizing the effective mode area of the waveguide might not provide the best measure of waveguide nonlinear parameter optimization [22]. Similarly, given the constraints arising from both processing and material properties of graphene, the optimization of the waveguide nonlinear parameter may not be derived by minimizing the effective area of the waveguide.

Processing constraints make it impossible to place the graphene layer in the center of the waveguide where the optical field is at its maximum. This implies that in silicon-graphene hybrid photonic waveguides, any graphene sheets reside in the region where the optical fields are evanescent, although this issue may be partially addressed via the use of dielectric loaded surface plasmon polariton waveguides. Furthermore, material constraints arise from the fact that graphene is grown layer by layer, with each layer being only 0.36nm thick. As a result, its total thickness can comprise only a negligible percentage of the waveguide structure.

Due to these considerations, the nonlinear index of the waveguides becomes a strongly varying function of the transverse profile, suggesting that a more appropriate parameter to maximize for optimizing nonlinear effects must involve the transverse dependence of $n_2(x,y)$. As a result of the aforementioned restrictions, a calculation of the waveguide effective area which assumes that most of the optical field resides within the active nonlinear region does not hold. We instead perform our optimization of the waveguides by maximizing the waveguide nonlinear parameter, which accounts for both the transverse dependence of the nonlinear index and the effective area. The nonlinear parameter is defined here by [23]:

#222438 - $15.00 USD Received 4 Sep 2014; accepted 4 Sep 2014; published 12 Sep 2014

$$\gamma = \frac{2\pi}{\lambda} \frac{\iint_D S_z^2 n_2(x,y) dx dy}{(\iint_D S_z dx dy)^2} \quad (4)$$

In the calculations that follow, n_2 used for graphene is 10^{-9} cm^2/W whereas that for Si is taken as 6 X 10^{-14} cm^2/W, within the range of experimentally reported values [24–28]. This particular value of n_2 for graphene was experimentally corroborated by nonlinear waveguide experiments that used graphene which was chemically doped for optical transparency at 1.55μm [13]. In [13], *p*-doped graphene with a doping density of 5 X 10^{12} cm^2 was experimentally shown to introduce minimal optical absorption to incident TE light while still retaining a large n_2 of 10^{-9} cm^2/W. It is further noted that the level of chemical doping required for optical transparency for the TE and TM mode is different [29]. We note further that graphene's nonlinearity is assumed here to be independent of the electric field polarization. However, recent papers report a slight difference between the nonlinear response graphene using incident light of different polarizations [30]. In particular, TE-polarized light was recently reported by Hong et. al to have ~30% higher nonlinear response compared to TM-polarized light. In other work, graphene's large n_2 has been shown to be able to support both TE and TM spatial solitons and graphene's nonlinearity is treated identically for polarizations [31, 32]. Since the observed differences in the nonlinear response of graphene for both polarizations are relatively small, we use the same value of n_2 for both polarizations for the purpose of our calculations. In the study that follows, it was found that although the graphene layer is very thin, the contribution of Si, SU8 [33] or SiO2 [22] to the nonlinear parameter is negligible in comparison for most of the configurations under study.

Our simulations use a commercially available Beam Propagation Method (BPM) to calculate modal profiles for the linear waveguide geometries. All calculations are performed using a free-space wavelength of 1550 nm. We define quasi-TE modes as those that are primarily polarized along the *x*-direction (along the dimension of the waveguide width), and quasi-TM modes as those that are primarily polarized along the *y*-direction (along the dimension of the waveguide height). Upon determination of the modal profile, the nonlinear parameter is evaluated using Eq. (4). In our simulations we assume that the negligible thickness of the graphene layer affects the linear modal profile minimally. The negligible impact of a graphene monolayer on the waveguide mode profile is further described in Refs 32 and 33. For the plasmonic waveguides, we used a mesh size of 0.18nm, which is half the thickness of graphene. For the photonic waveguides, we used a mesh size of 0.5nm which is larger than the thickness of graphene; the graphene layer is accounted for when computing the nonlinear parameter by performing an interpolation of the field profile to a smaller grid spacing. To ensure validity of this approximation, we sampled several points and calculated the nonlinear parameter using the interpolation method and using a grid size of 0.18nm and found that the values obtained were very similar.

3. Results

The first waveguide configuration considered was an SU-8 waveguide with an air cladding. Since SU8 is a polymer and may be easily spincoated, it is possible to fabricate the waveguide such that the graphene layer is positioned in the center of the SU8 waveguide core. Such an approach would allow the graphene layer to interact with the maximum of the electric field. The waveguide geometry was optimized in order to maximize the nonlinear parameter for both the fundamental TE and TM modes of the SU-8 waveguide. Results for the nonlinear parameter for the quasi-TE and quasi-TM modes are shown in Figs. 2(a) and 2(b) respectively.

For the quasi-TE mode, the maximum nonlinear parameter is reached for waveguides with height between 700 to 800 nm, and width between 1400 to 1600 nm. For the case of the quasi-TM mode (Fig. 2(b)), the largest nonlinear parameter is obtained at a waveguide

#222438 - $15.00 USD Received 4 Sep 2014; accepted 4 Sep 2014; published 12 Sep 2014

geometry of H = 1100nm and W = 700nm. The maximum nonlinear parameter is reached for larger heights and lower widths as compared to the TE mode case. SU8 has a negligible third order nonlinearity [30], and it is observed here that the inclusion of monolayer graphene within SU8 waveguides provides a means to generate a large nonlinear parameter on the order of that in conventional well-confined silicon-on-insulator waveguides.

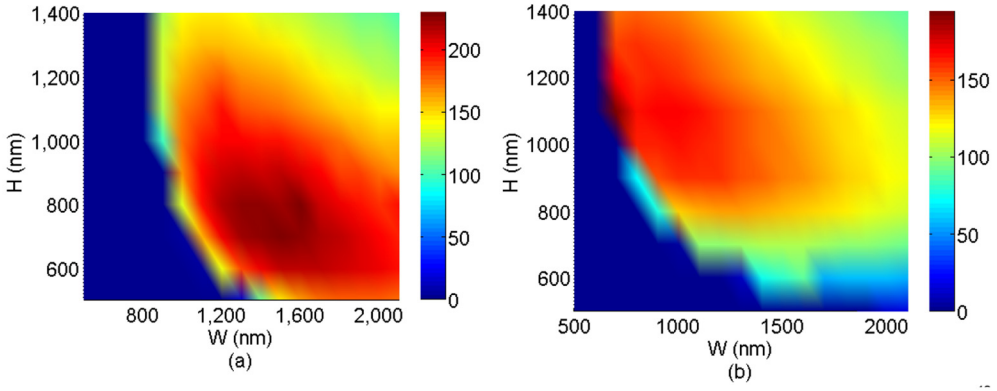

Fig. 2. Nonlinear parameter as a function of waveguide width and height for the SU-8 channel waveguide incorporating graphene for the (a) quasi-TE mode and (b) quasi-TM mode. Color bar shows the value of the nonlinear parameter (W^{-1}/m).

The second waveguide configuration under study consists of a silicon waveguide core with monolayer graphene on top of the silicon waveguide (see Fig. 1(b)). The waveguide over-cladding is air. The waveguide geometry was again optimized in order to maximize the nonlinear parameter for a range of widths and heights for both quasi-TE and TM modes.

The larger index contrast between core and cladding for the silicon waveguides allowed for well-confined propagating modes at smaller waveguide dimensions than for the SU-8 case. This in turn led to high values of the nonlinear parameter for the quasi-TE mode. Despite the fact that the graphene layer was no longer located at the region of highest intensity, the largest nonlinear parameter for the silicon channel waveguide exceeded 10^4 W^{-1}/m, about 40 times that for the SU-8 channel waveguide. This is attributed to the much larger magnitude of electric field in the Si-graphene boundary compared to the SU8-graphene boundary in the SU8 waveguide. In addition, it is expected that the geometries of SU8 waveguides that minimize the effective area will not lead to the largest effective nonlinearities. The reason for this is that the waveguides' nonlinear parameter in the SU8 waveguides is influenced by both the extent of field overlap with the graphene laterally and the tightness of field confinement within the SU8 waveguide. Since the index difference between SU8 and air is not very high, the field is not very tightly confined within the core and consequently, the lateral overlap of the optical field with graphene plays an important part. Therefore, the SU8 waveguide geometries leading to the maximum nonlinear parameters have a good balance of the two combined effects and not merely the geometries with the smallest effective areas.

Results for the quasi-TE mode for the graphene-Si waveguide are shown in Fig. 3(a). The highest nonlinear parameter occurs at a waveguide height of 70 nm and width of 350 nm. With these waveguide dimensions, the electric-field extends significantly outside of the core and into the graphene region. It is observed from Fig. 3(b) that the nonlinear parameter for the quasi-TM mode is two orders of magnitude lower than that for the quasi-TE mode. This is attributed to the reduced optical intensity in the silicon core and thus, reduced interaction of the optical field with the graphene layer compared with the quasi-TE mode. Consequently, the contribution of the graphene layer's nonlinearity to the nonlinear parameter in the quasi-

#222438 - $15.00 USD Received 4 Sep 2014; accepted 4 Sep 2014; published 12 Sep 2014

TM case is much lower, and becomes comparable to the contribution from the nonlinearity of the silicon core.

In silicon channel waveguides without a graphene monolayer, both theoretical and experimental results have shown that the optimum nonlinear parameter is achieved at a waveguide width and height of around 400 – 500nm and 200 – 300nm respectively [24, 25, 34]. These waveguide dimensions correspond to the region in which the effective area of the fundamental mode is smallest. In silicon-graphene hybrid channel waveguides supporting the quasi-TE mode as shown in Fig. 3(a), it is apparent that the waveguide configurations leading to the highest nonlinear parameters are not the ones which have the smallest effective areas. Conversely, waveguide configurations which have a larger effective area enable a larger amount of electric field to interact with the graphene layer. For example, the fundamental quasi-TE mode for a waveguide with h = 80nm and W = 350nm has a modal height (defined as the 1/e point of the magnitude of the electric field) of 1.5μm, and the magnitude of the E-field at center of the graphene layer is approximately 80% of its maximum within the waveguide mode. We note further that silicon waveguides as thin as 70nm have been demonstrated experimentally in [35] with losses as low as 0.3dB/cm. At larger waveguide heights, an increasing amount of the E-field resides within the core, and the intensity of the electric field interacting with the graphene monolayer decreases, leading to a reduction in the nonlinear parameter.

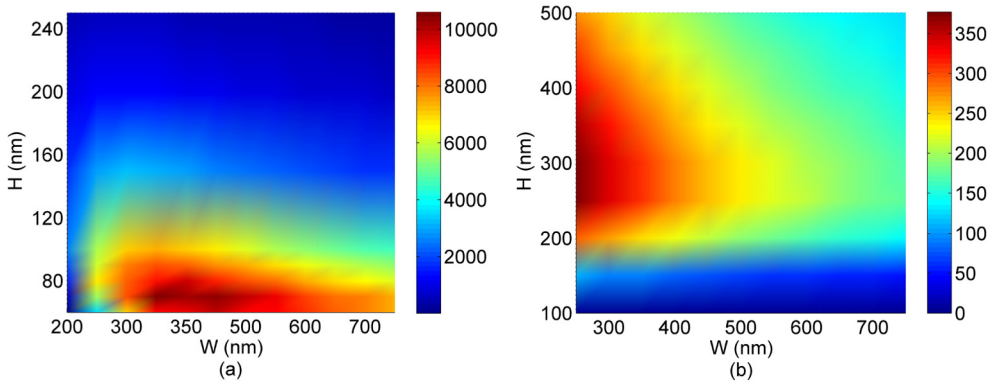

Fig. 3. Nonlinear parameter as a function of waveguide width and height for the graphene-Si channel waveguide incorporating graphene. (a) quasi-TE mode and (b) quasi-TM mode. Color bars show the magnitude of the nonlinear parameter (W^{-1}/m).

In surface plasmon polariton waveguides, the waveguide modal intensity is concentrated close to the boundary between the gold and dielectric region. This structure partially circumvents the fabrication limitations which result in graphene residing in the evanescent parts of the electric field in conventional photonic waveguides. Figure 1(c) shows the schematic of the waveguide under consideration. A silicon core is overlaid with a graphene monolayer followed by a 50nm thick layer of gold. The entire structure is overcladded with PMMA. PMMA is chosen as the overcladding as its index of 1.47 is close to that of SiO_2 (1.46) and it can be easily spincoated over the graphene – Si waveguide without damaging the graphene. This particular structure is studied because it is easily fabricated using conventional cleanroom microfabrication techniques and can integrate graphene with minimal difficulty. It is observed from Fig. 4 that the maximum nonlinear parameter for a fixed waveguide core height always occurs at W = 0.3μm.

For this particular case, the inclusion of the gold-layer results in an electric-field which is strongly confined in the gold-dielectric interface. Furthermore, the graphene layer is located in the region of maximum electric-field intensity at the gold-dielectric interface. Therefore, as a result of the tight optical confinement and strong overlap of the high-intensity region of the

#222438 - $15.00 USD Received 4 Sep 2014; accepted 4 Sep 2014; published 12 Sep 2014

E-field with the graphene layer, it is expected that the resultant nonlinear parameter of such structures will be much higher than that in the SU8 and Silicon photonic waveguides. Indeed, it is observed from Fig. 4 that the generated nonlinear parameters are up to an order of magnitude larger than that in the graphene-silicon waveguides.

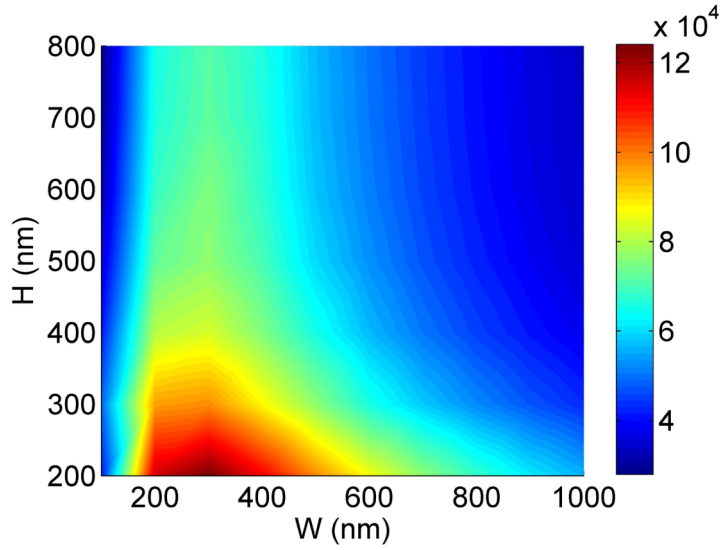

Fig. 4. Nonlinear parameter and (W^{-1}/m) as a function of waveguide width and height for silicon based dielectric loaded surface plasmon polariton waveguide incorporating graphene.

Overall, the two configurations providing the highest nonlinear parameters are the silicon channel waveguides supporting the quasi-TE mode and the DLSPP waveguides incorporating a graphene monolayer on the top. Although the DLSPP waveguides generate nonlinear parameters an order of magnitude higher than that of silicon channel waveguides, this structure also has the drawback of higher losses associated with the metal layer. Depending on the waveguide geometry, losses from the metal could be as high as tens of dB/cm. One approach which could be studied to mitigate this effect, is to explore the use of a buffer layer to reduce the deleterious effects of the lossy gold layer. Tradeoffs between the ultra-large nonlinear parameter possible in such waveguides incorporating graphene and the losses introduced from the gold layer must be balanced in order for the nonlinear strength to dominate and significant amounts of nonlinear phase to be acquired.

In any nonlinear platform, an important parameter is the nonlinear figure of merit, which is a measure of the nonlinear efficiency of the medium when both the nonlinear refractive index and nonlinear loss mechanisms are accounted for. This nonlinear figure of merit is given by the expression, $FOM_{NL} = n_2/(\beta_{TPA}.\lambda)$, where β_{TPA} is the two photon absorption coefficient [36, 37]. Graphene's large nonlinear refractive index also comes with an extremely large two photon absorption coefficient. For a graphene monolayer, the two photon absorption coefficient is described by the analytic expression [38], $\beta = \frac{4\pi^2}{\varepsilon_\omega \omega_4 \hbar^3}\left(\frac{v_F e^2}{c}\right)^2$, where ε_ω permittivity of graphene and ω is the angular frequency, $\hbar$ is the reduced Planck constant, v_F is the Fermi velocity, e is the electron charge and c is the speed of light in vacuum. At 1.55um, the TPA coefficient is calculated to be ~5cm/MW. Using graphene's $n_2 = 10^{-9}$ cm^2/W, its $FOM_{NL} = 1.29$. This figure is smaller than that in wide bandgap materials such as silicon nitride and silicon dioxide which have no two-photon absorption at 1.55μm, and only weaker multi-photon absorption terms [37]. The nonlinear figure of merit in graphene is however, higher than that in popular nonlinear optics platforms such as silicon,

#222438 - $15.00 USD Received 4 Sep 2014; accepted 4 Sep 2014; published 12 Sep 2014

which has a nonlinear figure of merit of ~0.3 at 1.55um [36]. Therefore, the integration of single or few-layer graphene can be used to increase the nonlinear performance of silicon-based waveguides.

To further increase the nonlinear parameter of graphene, waveguides with reduced group velocities can be used to increase the interaction of an incident E-field with the graphene layer. In highly dispersive waveguide platforms such as photonic crystal waveguides (PhC), the effective nonlinearity scales with a scaling factor, $S^2 = (n_g/n_0)^2$, where n_g is the group index of the waveguide mode and n_0 is the linear refractive index of the medium. Silicon PhC waveguides for example may be designed to have group indices as large as 38 [39], a value which augments the effective nonlinearity by a factor of ~120. In photonic waveguides with high confinement such as those based on the silicon on insulator platform, dispersion introduced by the waveguide geometry can also result in increases in n_g. Waveguides with weaker confinement for example have had group indices calculated to be close to 3.5 (e.g. 500nm by 120nm waveguide, $n_g = 3.5$ at 1.55 μm), whereas that for strong confinement was close to 4 (e.g. 500nm by 250nm waveguide, $n_g = 4.1$ at 1.55μm). Therefore, a similar scaling factor may be applied to silicon on insulator photonic waveguides under consideration here [40]. We note however that the silicon photonic waveguides under study here with the highest nonlinear parameters did not have strong confinement. Therefore, these waveguides would have group indices which are minimally augmented and consequently, generate smaller enhancements in the nonlinear parameter.

4. Conclusions

In this paper, we have studied the impact of mono-layer graphene on the nonlinear parameter in SU8 and silicon photonic waveguides, as well as DLSPP waveguides based on silicon on gold. It is shown that the minimization of the waveguide effective area in general is a poor indicator of high strong the waveguide nonlinear parameter is. Where graphene may be located at the region of maximum E-field, such as at the center of the SU8 waveguide and in the metal-dielectric interface in DLSPP waveguides, better correlation is achieved between the minimum waveguide effective area and maximum nonlinear parameter. In all waveguide configurations, it is observed that a single layer of graphene can augment the nonlinear parameter of the waveguide by more than 2 orders of magnitude. Optimal waveguide geometries yielded nonlinear parameters exceeding 10^4 W^{-1}/m in silicon photonic waveguides, two orders of magnitude larger than those without the graphene monolayer present. The nonlinear parameter for the quasi-TM mode was much lower than that for the quasi-TE mode, as a result of the extremely low magnitude of E-field at the core-cladding boundary where the graphene was located. In the quasi-TM case in the silicon photonic waveguides, the contribution to the overall nonlinear parameter from the silicon core is comparable to that from the graphene mono-layer. Optimal waveguide geometries in the silicon-gold DLSPP waveguide yielded nonlinear parameters exceeding 10^5 W^{-1}/m, 3 orders of magnitude larger than that in silicon photonic waveguides without mono-layer graphene. Strategies to mitigate nonlinear losses introduced by the lossy gold layer can be employed to ensure that the ultra-large nonlinear parameter obtained from the introduction of the graphene layer dominates and substantial nonlinear phase acquisition can be obtained.

The ultra-large nonlinear parameters which are enabled in graphene-integrated photonic and DLSPP waveguides make such waveguides promising platforms for nonlinear integrated optics at ultra-low powers such as soliton formation [32], supercontinuum generation and optical parametric amplification, and for previously unobserved nonlinear optical effects to be studied in a waveguide platform.

#222438 - $15.00 USD Received 4 Sep 2014; accepted 4 Sep 2014; published 12 Sep 2014

Acknowledgments

This work was supported by the MOE ACRF Tier 2 research grant, SUTD-MIT International Design Center and the SUTD-ZJU collaborative research grant. Discussions with Dr. Kelvin J. A. Ooi are greatly appreciated.

#222438 - $15.00 USD Received 4 Sep 2014; accepted 4 Sep 2014; published 12 Sep 2014